Semicond. Sci. Technol. **23** (2008) 015017 (5pp) doi:10.1088/0268-1242/23/1/015017

SIMS analysis of intentional *in situ* arsenic doping in CdS/CdTe solar cells

R L Rowlands, S J C Irvine, V Barrioz, E W Jones and D A Lamb

School of Chemistry, University of Wales, Bangor, Gwynedd, LL57 2UW, UK

E-mail: chp01a@bangor.ac.uk

Received 6 September 2007, in final form 8 November 2007
Published 13 December 2007
Online at stacks.iop.org/SST/23/015017

Abstract

A series of CdTe/CdS devices with different tris(dimethylamino)arsine (TDMAAs) partial pressures were grown by metal organic chemical vapour deposition (MOCVD) to investigate the incorporation of arsenic into the bulk. Characterization of the growth layers using secondary ion mass spectrometry (SIMS) showed arsenic concentrations ranging from 1×10^{16} to 1×10^{19} atoms cm^{-3}. A square law dependence of arsenic concentration on the TDMAAs vapour concentration was observed. A reaction mechanism for the decomposition of TDMAAs precursor via dimerization is presented and discussed in terms of reaction kinetics.

1. Introduction

Intentional doping of both sides of the p–n junction in metal organic chemical vapour deposition (MOCVD) grown CdTe/CdS material was first demonstrated by Berrigan *et al* [1]. A statistical methodology used in recent work highlighted arsenic concentration in the CdTe layer as an important parameter in improving photovoltaic (PV) device characteristics [2, 3]. In addition to the four main growth parameters, temperature, deposition time, pressure and site specificity, the chemical nature and behaviour of the precursor is also crucial. Doping is a complex process and effective control of this operation requires an understanding of several factors: precursor decomposition, transport to the surface, surface reactions, gas phase reactions and surface sites.

Ghandhi *et al* doped epitaxial films grown onto single-crystal CdTe substrates using arsine (AsH_3) [4]. Other arsenic precursors have been investigated in detail for the growth of III–Vs, including tertiarybutylarsine (TBA) [5] and trimethylarsine (TMA) [6]. The choice of precursor can affect homogeneity, morphology and contamination of the growth layer. Alternative organometallic (OM) precursors have interesting decomposition properties, which can provide information on growth stability issues including thermal stability, pre-reaction and precursor ratio of the OMs. Pre-reactions are important as they can cause difficulties in controlling the growth defect chemistry and dopant incorporation. The precursor ratio is an important factor that can greatly affect the stoichiometry.

Early work on MOCVD growth mechanisms concentrated on the pyrolysis of the organometallics. In this work tris(dimethylamino)arsine (TDMAAs) was the selected precursor. TDMAAs pyrolyses at lower temperatures than arsine and TBA with 50% decomposition achieved at 350 °C, leading to atomic arsenic [7]. Although pyrolysis data are crucial, other parameters including surface catalysis and surface kinetics can dominate. Easton *et al* showed that the decomposition of diethyltellurium (DETe) was significantly affected by surface specificity [8].

Lee *et al* noticed the presence of a stable tetramer below 250 °C at low arsenic concentrations; at high arsenic concentrations they observed that the tetramer transforms into two neutral dimers [9]. The complex material structure of polycrystalline PV devices makes the separation of the effects of growth parameters increasingly difficult. Characterization of these materials plays an important role in understanding the effects of dopants within the structure.

2. Experimental details

CdTe/CdS structures were grown using atmospheric pressure MOCVD, onto commercially available ITO/glass substrates from Delta Technologies Ltd. The organometallic precursors for Cd, S and Te were dimethylcadmium (DMCd), ditertiarybutylsulphide (DTBS) and diisopropyltelluride (DIPTe), respectively. The CdTe layers were *in situ* arsenic doped using tris(dimethylamino)arsine (TDMAAs) in a double dilution line arrangement with different partial pressures

Table 1. Summary of the experimental conditions used for the SIMS depth profiling.

Instrument	Cameca ims 4f
Primary ion species	Cs^-
Primary ion energy	10 keV
Primary ion current	70 nA
Raster size	200 μm
Secondary ions	Negative
Transfer lens	150 μm
Analysed area	30 μm
Contrast aperture	No 3
Mass resolution	250

ranging from 3×10^{-9} to 1×10^{-6} atm. A 240 nm window layer of CdS was deposited at 315 °C with a growth rate of 0.14 nm s^{-1}. The partial pressures of DTBS and DMCd were 2.7×10^{-4} atm obtaining a II:VI of 1. A 2 μm CdTe absorber layer was deposited at 390 °C with a growth rate of 0.44 nm s^{-1}. A DIPTe partial pressure of 1.1×10^{-4} atm and a DMCd partial pressure of 2.0×10^{-4} atm were used creating a II:VI of 1.8. The arsenic concentrations within the growth layers were determined by secondary ion mass spectrometry (SIMS). Samples were supplied for SIMS analysis after a chemical polish with 0.25% bromine in methanol, which reliably removes ~1 μm of material and smooths the surface.

SIMS depth profiles were run on a Cameca ims 4f instrument with a Cs^+ 10 keV primary ion beam from the CdTe back surface through to the TCO. The ion counts were calibrated into concentrations (atoms cm^{-3}) using supplied reference samples of arsenic implants in CdTe layers on glass substrates. The depth scales were determined by measuring the sputtered crater depth on the reference samples by interference microscopy assuming a uniform erosion rate. The main experimental conditions for the SIMS profiles are summarized in table 1.

The species investigated were matrix elements Cd, Te and S, and the intentional dopant arsenic. The detection limit of arsenic was in the region of 1×10^{16} atoms cm^{-3}. All of the devices submitted for SIMS analysis were from the downstream end of the susceptor.

3. Results and discussion

3.1. Arsenic doping

The Taguchi methodology [2, 3] used in previous work highlighted arsenic concentration as an important growth parameter in potentially improving device characteristics. Control over the dopant incorporation is therefore a critical step. Figure 1 shows a schematic of the doping sequence for arsenic in CdTe.

At the surface of the CdTe layer there are tellurium vacancies, which can be filled by arsenic causing p-type doping. A series of CdTe/CdS structures were grown with different TDMAAs partial pressures to monitor the control and incorporation of arsenic into the bulk. The arsenic concentrations within the CdTe layers were determined by SIMS depth profiling.

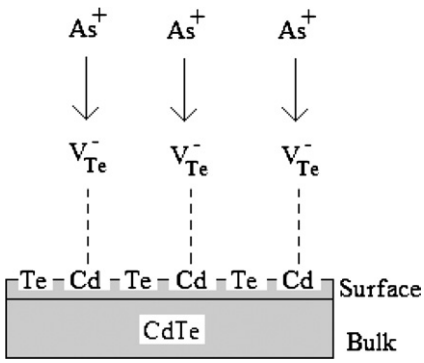

Figure 1. A schematic of the doping sequence of arsenic in CdTe.

The device structures with TDMAAs partial pressures of 3×10^{-8} and 3×10^{-9} atm shown in figure 2 yield arsenic concentrations in the background region indicating a detection limit of 1×10^{16} atoms cm^{-3}; therefore, the profiles cannot be clearly seen. This indicates that the detection limit of the Cameca ims 4f instrument is of the order of 1×10^{16} atoms cm^{-3}. The sulfur profile rises as the ion beam mills through the CdTe/CdS interface into the CdS layer. The arsenic profile also rises towards the interface indicating that arsenic may be diffusing through the absorber layer towards the interface, most likely along the grain boundaries.

SIMS depth profiles of higher TDMAAs partial pressures ranging from 6×10^{-8} up to 1×10^{-6} atm, presented in figure 3, clearly show concentrations above the background. The arsenic concentrations in the layers range from 1×10^{18} to 1×10^{19} atoms cm^{-3}. Each device structure has a uniform arsenic profile throughout the CdTe layer with minimal noise. The rise in the sulfur trace as the ion beam moves through the CdTe/CdS interface into the CdS layer is visible in each depth profile.

3.2. Arsenic incorporation

A plot of the logarithms of TDMAAs partial pressure against the logarithms of arsenic concentration in the CdTe layers presented in figure 4 shows a linear trend above the detection limit of the Cameca ims 4f instrument.

This trend can be explained in terms of kinetics. Assuming the rate law for a reaction with reactive species, A, in isolation is

$$r = k[A]^a, \tag{1}$$

then the initial rate r_0 is given by the initial value of the concentration of A as expressed in equation (2). For these experiments this can be assumed to be the inlet concentration of TDMAAs:

$$r_0 = k[A]_0^a. \tag{2}$$

Taking logarithms

$$\log r_0 = \log k + a \log[A]_0. \tag{3}$$

Therefore for a series of initial concentrations, a plot of the logarithms of the initial rates against the logarithms of the initial concentration should be linear with slope a. In this work

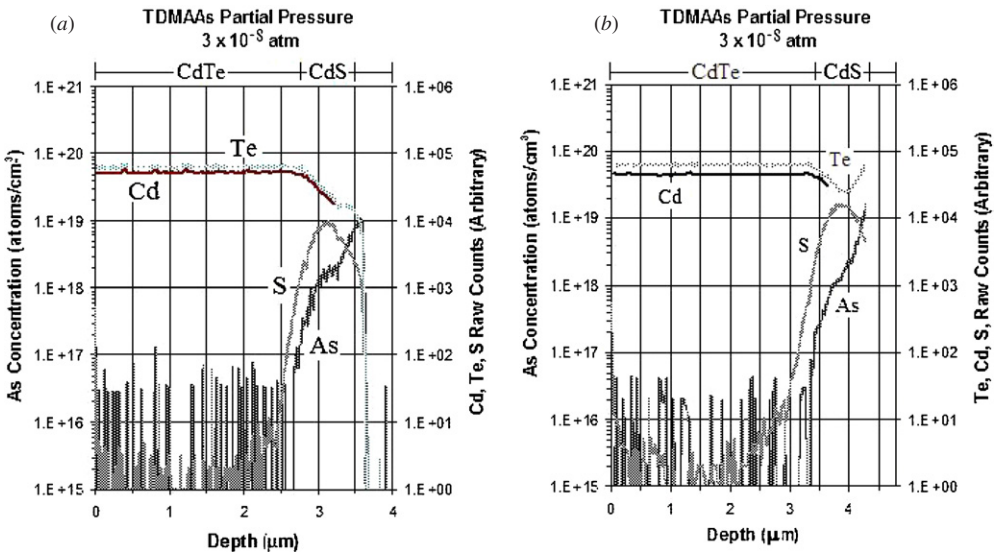

Figure 2. SIMS depth profiles of device structures from the CdTe surface to the TCO with TDMAAs partial pressures of (*a*) 3×10^{-8} atm and (*b*) 3×10^{-9} atm indicating a detection limit of 1×10^{16} atoms cm^{-3}.

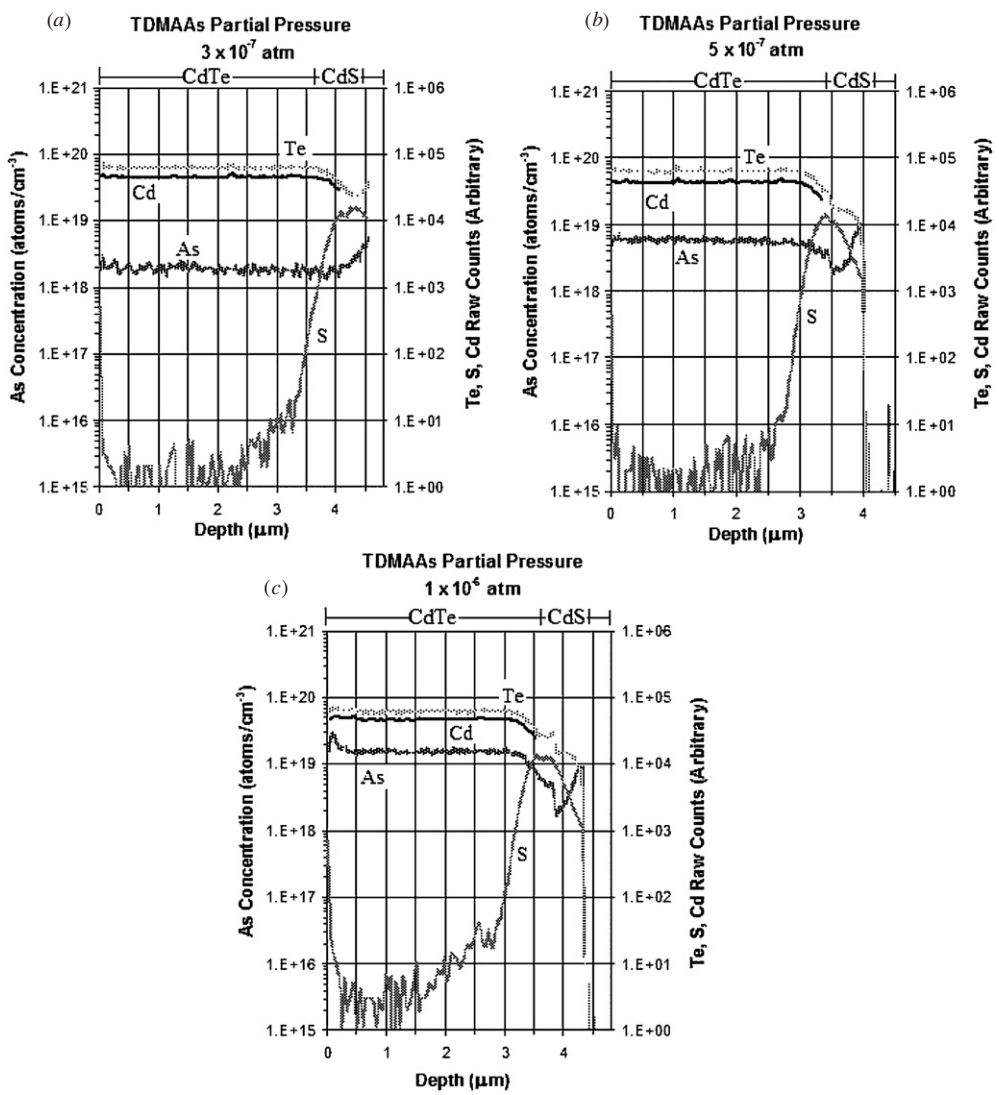

Figure 3. SIMS depth profiles of device structures from the CdTe surface to the TCO with TDMAAs partial pressures of (*a*) 3×10^{-7} atm, (*b*) 5×10^{-7} atm and (*c*) 1×10^{-6} atm corresponding to arsenic concentrations up to 1.5×10^{19} atoms cm^{-3}.

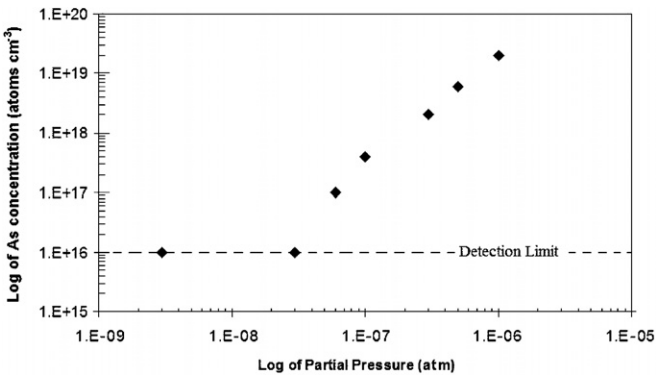

Figure 4. A plot of the logarithms of TDMAAs partial pressure against the logarithms of arsenic concentration in the bulk.

the rate of arsenic incorporation is taken as the concentration of arsenic in the layer, as the growth rate of CdTe was independent of As concentration. The linear trend has a slope of $a = 2$, which can be described as a square law dependence of arsenic incorporation into the bulk material on partial pressure indicating that the reaction follows second-order kinetics.

The growth rate is proportional to the flux of atoms being transported, by diffusion through the gas phase to the interface, and is equivalent to the flux of atoms crossing the interface to the solid. Some of the key stages involved in arsenic incorporation into the bulk are listed below:

(1) Transport of the organometallics.
(2) Decomposition of the organometallics.
(3) Adsorption to the surface.
(4) Desorption.

The reactions at the surface and in the gas phase will both occur during growth. Which process dominates is determined by factors including temperature at the surface, temperature in the gas and site specificity. The precursors will adsorb onto the surface via chemisorption or physisorption. It can be assumed that there are a fixed number of reactive sites upon the surface, which an atom or molecule can absorb to. Once a site is filled, a second molecule cannot absorb there. The number of atoms that desorb from the surface is dependent on the surface concentration at a constant temperature. The maximum amount of arsenic incorporation that can be achieved is the amount that would establish equilibrium assuming that the molar concentration is constant in the gas stream.

Previous SIMS characterization showed a saturation point above a partial pressure of 1×10^{-6} atm, which would be indicative of a limit to the incorporation of As in these layers. This is the solubility limit and saturation of the bulk solubility will lead to a saturation point for the incorporation of arsenic into the bulk.

3.3. Possible decomposition route for TDMAAs

The experimental data show second-order kinetics. This requires a rate-limiting step that is of second order.

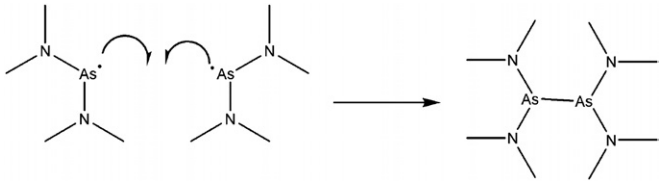

Figure 5. The proposed dimerization reaction of the second-order rate-limiting step and the resulting arsenic dimer structure.

One possible explanation for second-order kinetics is the decomposition of TDMAAs via dimerization. A potential mechanism for the decomposition of TDMAAs in the gas phase is presented below. The proposed mechanism is a chain reaction initiated by homolysis or reaction with hydrogen radicals produced during the decomposition of DMCd. Once initiated, the hydrogen radicals are replenished during the decomposition of TDMAAs in steps 2 and 4:

(1) $\mathrm{TDMAA_s + H^{\cdot} \rightarrow ((CH_3)_2N)_2AsCH_3N^{\cdot} + CH_4}$.
(2) $\mathrm{((CH_3)_2N)_2AsCH_3N^{\cdot} + H_2 \rightarrow ((CH_3)_2N)_2AsCH_3NH + H^{\cdot}}$
(3) $\mathrm{((CH_3)_2N)_2AsCH_3NH + H^{\cdot} \rightarrow ((CH_3)_2N)_2AsNH^{\cdot} + CH_4}$.
(4) $\mathrm{((CH_3)_2N)_2AsNH^{\cdot} + H_2 \rightarrow ((CH_3)_2N)_2AsNH_2 + H^{\cdot}}$
(5) $\mathrm{((CH_3)_2N)_2AsNH_2 + H^{\cdot} \rightarrow ((CH_3)_2N)_2As^{\cdot} + NH_3}$.

Bond strength data indicate that the N–C bonds are the weakest in the precursor (305 kJ mol^{-1}). It is conceivable that the methyl group is removed, producing a nitrogen radical species and methane as shown in step 1. Once both methyl groups have been removed from the nitrogen (steps 2–4), the As–N bond (489 kJ mol^{-1}) will break, resulting in an arsenic radical species and a stable leaving group, ammonia (step 5). The removal of the remaining dimethylamino groups will become less favourable via the same pathway as the bond strengths will increase as groups are removed despite the possibility of stable leaving groups. This reaction pathway is supported by a study showing that methyl radicals are not produced during the decomposition of tris(dimethylamino)antimony (TDMASb) [10].

Step 6 shows a reaction step proposed by Salim *et al* for the initial decomposition of tris(dimethylamino) As, P and Sb species via reaction initiated by homolysis or reaction with hydrogen radicals [11]:

(6) $\mathrm{[(CH_3)_2N]_3As + H^{\cdot} \rightarrow [(CH_3)_2N]_2As^{\cdot} + (CH_3)_2NH}$.
Both routes result in the same arsenic radical species with two dimethylamino groups which can then undergo dimerization as shown in step 7.
(7) $\mathrm{2 \times ((CH_3)_2N)_2As^{\cdot} \rightarrow ((CH_3)_2N)_2As \times As(N(CH_3)_2)_2}$.

It is proposed that the dimerization of the bis-dimethylaminoarsenic species occurs before subsequent dimethylamino groups can be removed. The proposed dimer structure is shown in figure 5.

The As–As bond is stronger than the As–N bond and therefore the removal of the remaining dimethylamino groups will occur more readily in an arsenic dimer species. The experimental data show a square law dependence, indicating that the rate-limiting step is of second order. This shows that

for decomposition to occur a dimer has to form which provides an explanation for the experimental evidence of a second-order rate law.

It is unlikely that a bulky species adsorbs to the surface because many surface reactive sites would be blocked, hindering the CdTe growth and reducing the CdTe growth rate. The observed growth rate of the CdTe remained constant throughout this work and is evidence that a less bulky group adsorbs to the surface. It is probable that the final species adsorbing to the surface is an arsenic dimer species (As_2) leading to monoatomic arsenic [7].

4. Conclusions

The arsenic concentrations within the CdTe layers were measured using SIMS depth profiling and ranged from 1×10^{16} to 1×10^{19} atoms cm^{-3}. The arsenic profiles were flat and continuous through the bulk. A plot of the logarithms of arsenic partial pressure against the logarithms of arsenic concentration in the bulk produced a linear trend with a slope of 2, indicating that the incorporation of arsenic into the bulk follows second-order kinetics. It is proposed that the rate-limiting step is the formation of the $(CH_3)_2N)_2AsAs(N(CH_3)_2)_2$ dimer. The uniform growth rate is evidence that a less bulky group such as arsenic dimers (As_2) adsorbs on the CdTe surface. Saturation at TDMAAs partial pressures greater than 1×10^{-6} atm is most likely due to saturation in the bulk solubility.

Acknowledgments

The authors gratefully acknowledge the financial support of EPSRC (PV SuperGen—PV Materials for the 21st Century) and CSMA-MATS, UK, and Loughborough Surface Analysis for the SIMS depth profiles.

References

[1] Berrigan R A, Irvine S J C and Stafford A 1998 *J. Cryst. Growth* **195** 718–24
[2] Barrioz V, Rowlands R L and Irvine S J C 2005 *20th EUPVSEC (Barcelona, 6–10 June 2005)* p 1918
[3] Barrioz V, Rowlands R L, Jones E W, Irvine S J C, Zoppi G and Durose K 2005 *Mat. Res. Soc. Symp. Proc.* **865** 67–72
[4] Ghandhi S K, Taskar N R and Bhat I B 1987 *Appl. Phys. Lett.* **50** 900
[5] Chu S S, Chu T L, Green R F and Cerny C 1991 *J. Appl. Phys.* **69** 8316
[6] McCluskey M D, Haller E E, Zach F X and Bourret-Courchesne E D 1996 *Appl. Phys. Lett.* **68** 3476–8
[7] Bevan M J, Shih H D, Dodge J A, Syllaias A J and Weirauch D F 1998 *J. Electron. Mater.* **27** 769–71
[8] Easton B C, Maxey C D, Whiffin P A C, Roberts J A, Gale I G, Grainger F and Capper P 1991 *J. Vac. Sci. Technol.* B **9** 1682
[9] Lee T S, Garland J, Grein C, Sumstine M, Jandeska A, Selamet Y and Sivananthan S 2000 *J. Electron. Mater.* **29** 869
[10] Wang C A 2004 *J. Cryst. Growth* **272** 664–81
[11] Salim S, Lim C K and Jensen K F 1995 *Chem. Mater.* **7** 507–16